Supporting Information

A hexanuclear Cu(I) cluster supported by cuprophilic interaction: Effects of aromatics on luminescence properties

Anindita Chakraborty,[a#] Ramachandran Krishna Kumar, [a#] Sharma SRKC Yamijala,[b] Swapan K. Pati [b] and Tapas K. Maji* [a]

[#]These authors contributed equally

[a] *Molecular Materials Laboratory, Chemistry and Physics of Materials Unit, Jawaharlal Nehru Centre for Advanced Scientific Research, Jakkur, Bangalore – 560 064, India. *E-mail: tmaji@jncasr.ac.in, Phone: +91 80 2208 2826, FAX: +91 80 2208 2766*

[b] *Theoretical Science Unit, Jawaharlal Nehru Centre for Advanced Scientific research, Jakkur, Bangalore – 560 064, India.*

Materials required: All the reagents were purchased from Aldrich Chemical Co. Inc. and Spectrochem Pvt. Ltd., Mumbai, India. All the chemicals were use without further purification.

Physical measurement:

Elemental analyses were carried out using a Perkin Elmer 2400 CHN analyzer. Powder X-ray diffraction (PXRD) patterns were recorded on a Bruker D8 Discover instrument using Cu–Kα radiation. IR spectra were recorded on a Bruker IFS 66v/S spectrophotometer using KBr pellets in the region 4000–400 cm^{-1}. UV-Vis spectra were recorded on a Perkin Elmer Model Lambda 900 spectrophotometer and fluorescence spectra were recorded on a Perkin Elmer Model LS 55 spectrophotometer. The time drive option in the instrument has been used for time dependent fluorescence study. The fluorescent quantum yields were measured using an absolute photoluminescence quantum yield measurement system.

Single-crystal X-ray Diffraction:

X-ray single-crystal structural data of **1** was collected on a Bruker Smart–CCD diffractometer equipped with a normal focus, 2.4 kW sealed tube X-ray source with graphite monochromated

Mo–Kα radiation (λ = 0.71073 Å) operating at 50 kV and 30 mA. The SAINT program[1a] was used for integration of diffraction profiles and absorption correction was made with SADABS[1b] program. All the structures were solved by SIR 92[1c] and refined by full matrix least square method using SHELXL 97[1d]. All the non-hydrogen atoms were refined anisotropically and all the hydrogen atoms were fixed by HFIX and placed in ideal positions. All calculations were carried out using SHELXL 97, PLATON[1e] and WinGX system, Ver 1.70.01.[1f]

Crystal data of 1: empirical formula = $C_{60}H_{42}Cu_6O_{18}$, M = 1432.24, Triclinic, space group *P-1*, a = 11.0572(17) Å, b = 11.7719(11) Å, c =12.2096(17) Å, α=69.518(11)°, β=67.483(14)°, γ=65.832(12)°, V= 1303.8(3)Å^3, T=293K, Z=1, D_{calcd} = 1.824 g/cc, *F(000)*=720, R_{int}=0.0534, R_w =0.1616 for 3451 reflections with $I \geq 2\sigma(I)$, *GOF*=1.05, $\Delta\rho$ max/min [e Å^{-3}]= 0.61/-0.81.

Study of vapour sensing: To study the vapour sensing property, thin layers were prepared on quartz slides. Double-sided tape was applied to lower part of a clean and dried quartz slide and then peeled off after few minutes. The powder sample of compound **1** was then spread evenly onto the glued surface of the slide and a thin continuous layer of sample was thus formed.

For the solid analytes (1,2-DNB, DNT and NM), 10 mmol of each were placed in open glass vials (20 ml) which were placed into capped (500ml) glass bottles for ten days to ensure that the equilibrated vapor pressure of each analytes was reached. Similarly for the liquid sample (NB, toluene, *o*-xylene, *p*-xylene), 10 mmol of each was taken and the previous procedure was followed. The emission spectrum of the thin layer of the parent compound (**1**) was collected before placing the slide into the bottles containing the particular analyte. After definite exposure time, the slide was taken out and immediately the emission spectrum was recorded. New slides with a thin layer were used for each of the experiment.

Computational Details:

Geometry optimizations and UV-Visible spectra of all the molecules have been calculated using density functional theory (DFT) and Time-dependent DFT (TDDFT) methods, respectively, as implemented in Gaussian software[2]. We have used B3LYP exchange correlation functional, with LANL2DZ basis-set for copper atoms and 6-31g(d) basis-set for other atoms, in all our

calculations. Previously, it has been shown that TDDFT at B3LYP/6-31g(d) level of theory will give good results for low-energy excited states of larger molecules.[3]

Detailed discussion of computation results:

We have performed DFT/TDDFT calculations in order to understand both the nature of the excited state emission and also to know the possible reasons for the luminescence quenching/enhancing of the parent compound in the presence of analytes. First, hydrogen atoms of the experimentally obtained structure have been optimized with a singlet multiplicity. Next, absorption spectra (for first 50 singlet states) of this optimized structure have been calculated. Fig. S7 shows both the experimental and the calculated UV-visible spectra and it is clear that the calculated spectrum has captured the main features of the experimental spectrum. Calculated spectrum is mainly spanned over 260-340 nm region (at this level of theory), with a large number of high intense peaks being located mainly in the 260-310 nm region. Analyzing the excitations (whose oscillator strength is more than 0.01) we found that the excitations have ligand to metal charge-transfer (LMCT) character (see Table S2) as well as ligand to ligand charge-transfer (LLCT) and metal-metal charge-transfer (MMCT) characteristics. These preliminary calculations show that the transitions having high oscillator strengths (for example, see transitions 8 and 19 of Table S2) are mainly of hybrid character (i.e. a mixture of LMCT, MMCT and LLCT).

Next, we have followed Angelis *et. al*[4a] and Perruchas *et. al*[4b] to calculate the emission of the parent-compound **1**. We have optimized the H-atom positions of the experimental structure and found it to exist in a singlet state. We then optimized this structure considering a triplet (T1) spin state at B3LYP/6-31g(d) level of theory and found a single state (S1) is at a lower energy, in the same geometry as the triplet state (T1). However, if we completely optimize the complex in the singlet state then the system has the lowest energy (S0). Given the singlet and triplet state energies, as shown in the Table S3, the calculated emission wavelength (~ 587 nm) (energy difference between T1 and S1 states[4]) is very close to the experimental emission wavelength (~ 560 nm). Considering that this emission corresponds to the experimental emission peak[4], we have calculated the electron density difference map (EDDM) between these triplet (T1) and singlet states (S1) (Fig. 2 in main manuscript), to understand the nature of emission. Clearly, this map established cluster centered emission in this compound.

Finally, to understand the reason for the fluorescence quenching and enhancing in the presence of electron withdrawing and electron rich compounds respectively, we have calculated the HOMO and LUMO levels of all the compounds optimized at the same level of theory (B3LYP/6-31g(d)). The respective energy levels are plotted in Fig. S17. Clearly, the LUMO of all compounds having electron donating groups lie above the LUMO of parent-compound while for compounds with electron withdrawing groups, the LUMOs lie below the LUMO of **1**. This result is in accordance with the suggested donor-acceptor electron transfer mechanism in excited state.

Synthesis of 4,4′,4′′-[1,3,5-phenyl-tri(methoxy)]-tris-benzoic acid (L)

Methyl-4-hydroxy benzoate (1 g, 6.57 mmol), potassium carbonate (2.890 g, 20.1 mmol) and potassium iodide (0.085 g, 0.51 mmol) were heated in 30 mL DMF at 100 °C for 2 hours in nitrogen atmosphere. Solution of 1,3,5-Tris(bromomethyl)benzene (0.500 g, 1.4 mmol) in 20 mL DMF was then added dropwise to the above heated mixture and the mixture was heated for 4 hours at 100 °C. After cooling to room temperature, 100 mL of distilled water was added to it. The precipitate formed was filtered, washed with cold distilled water and air dried to get white solid of the ester 4,4′,4′′-[1,3,5-phenyl-tri(methoxy)]-tri-methyl benzoate (Scheme S1).

For the ester hydrolysis, to 4,4′,4′′-[1,3,5-phenyl-tri(methoxy)]-tri-methyl benzoate (~500 mg), 40 mL of MeOH and 1 g of sodium hydroxide dissolved in 10 mL of water was added in a round bottomed flask. The reaction mixture was then stirred at 50 °C for 12 hours. After cooling to room temperature, the solution was placed in an ice bath and acidified with 6N hydrochloric acid. The precipitate formed was then filtered, washed with cold distilled water and dried. A solid of 4,4′,4′′-[1,3,5-phenyl-tri(methoxy)]-tris-benzoic acid ligand was obtained, which was characterized by NMR (Fig. S1).

Synthesis of $\{Cu_3(L)_2\}_2$ (1):

Compound **1** was synthesized by self-assembly between Cu(II) ion and the tripodal ligand L employing solvothermal condition. $Cu(NO_3)_2.2.5H_2O$ (0.075 mmol) and L (0.05 mmol) in were taken in a 23 ml Teflon bomb. To this solution 6 ml DMF was added and the solution was stirred for 10 minutes. The Teflon bomb was kept at 120°C for 2 days. After completion of the reaction, the bomb was cooled to RT for 12 hour. Colorless block shaped crystals along with powder were

formed. CHN analysis of **1**; calculated: C: 50.317; H: 2.956. Found: C: 50.0859; H: 2.9051. Infrared spectrum of compound **1** is shown as Fig. S2. Selected IR data (KBr, cm^{-1}); 1603 s, 1531 m, 1414 s, 1385 s, 1218 m, 1176 m, 849 s, 771 m. Fig. S3 represents the Powder XRD of as-synthesized and simulated one, which suggests high phase purity of the sample.

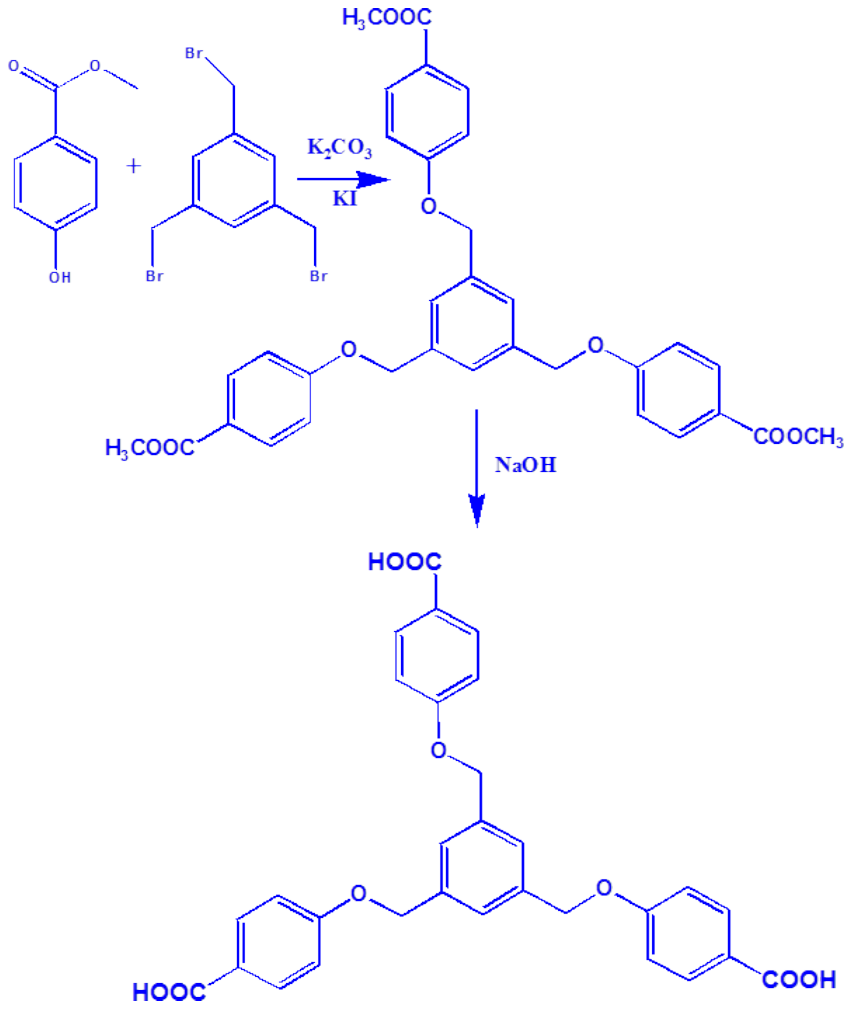

Scheme S1: The reaction pathways of the ligand synthesis.

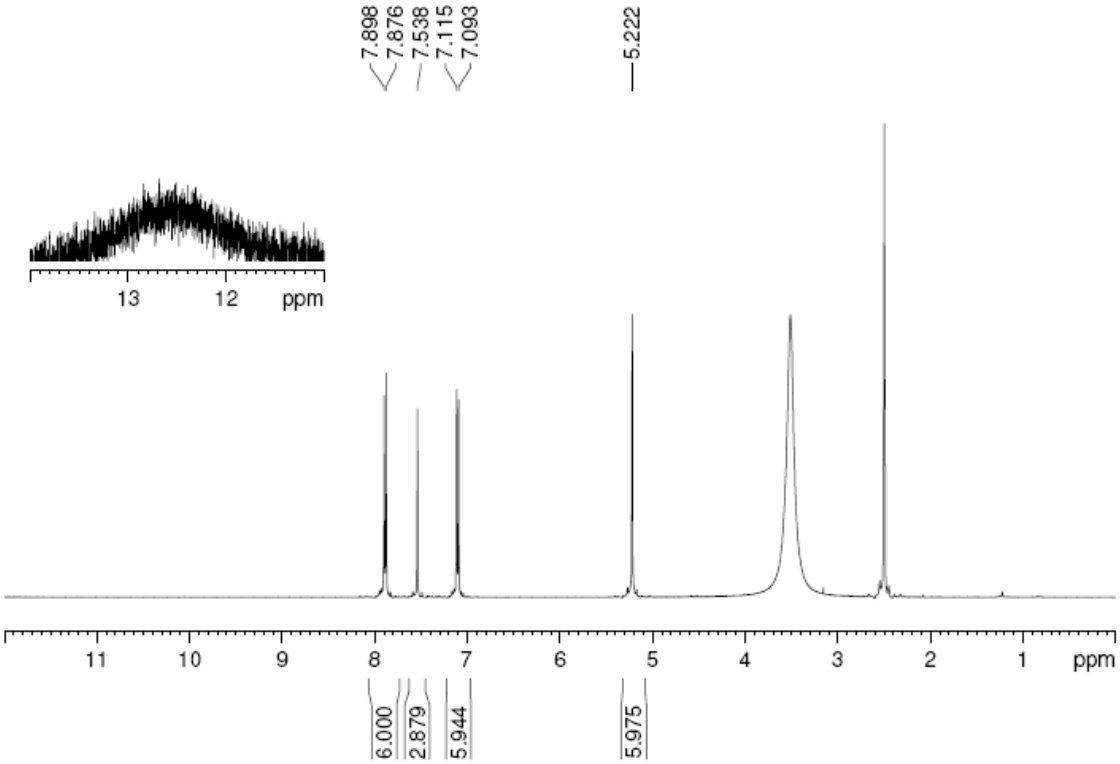

Fig. S1: NMR spectrum of L. The inset shows the presence of acidic proton of the carboxylic acid group.

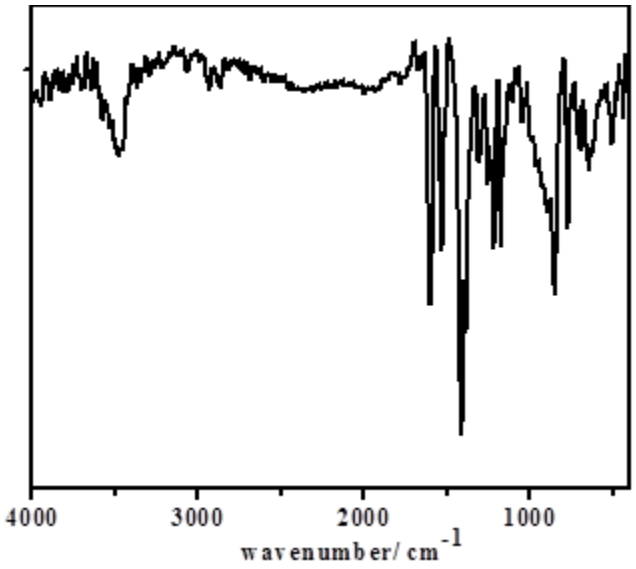

Fig. S2: IR spectrum of the **1**.

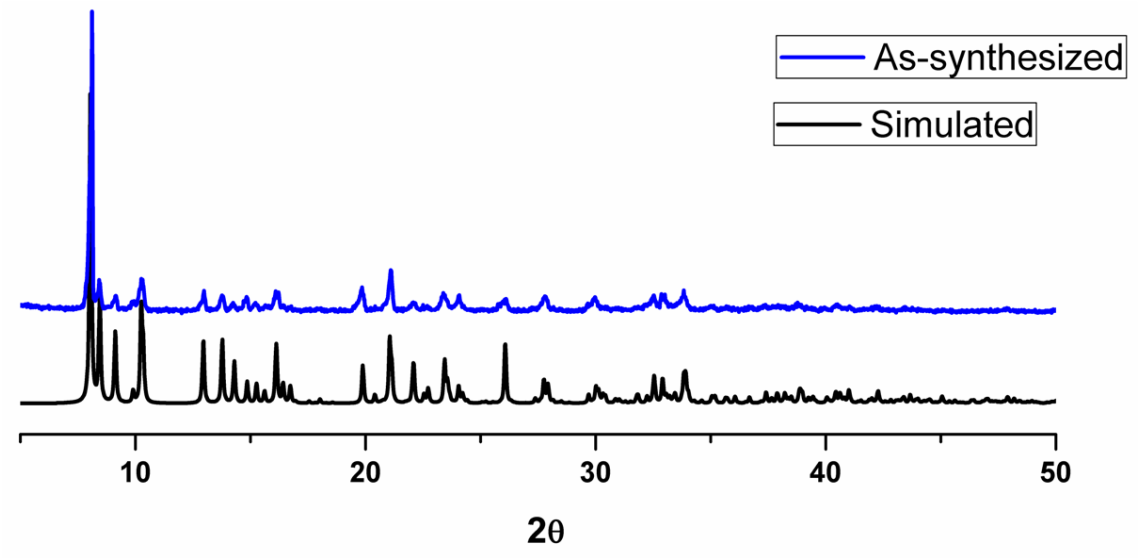

Fig. S3: Powder XRD of the simulated and as-synthesized sample.

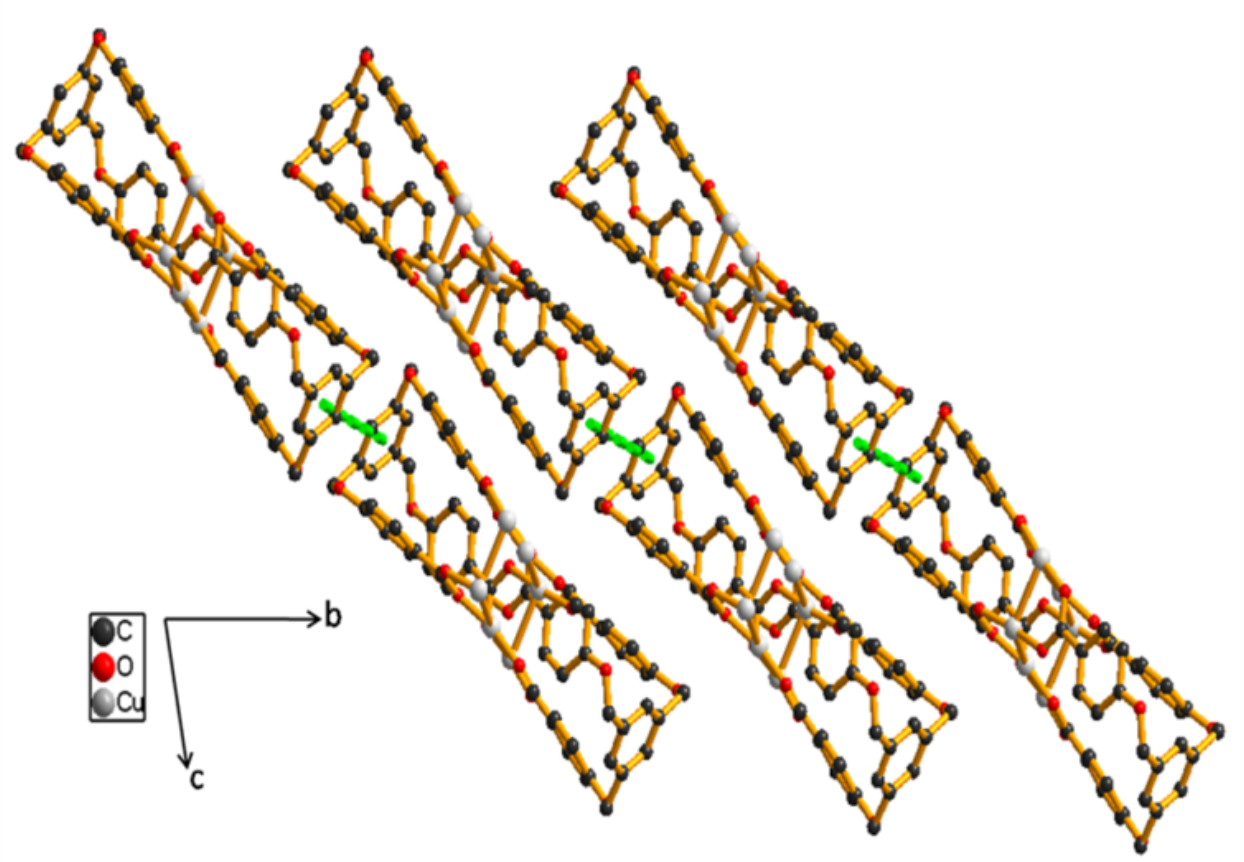

Fig. S4: The packing of clusters in one dimension, a view along crystallographic *a* direction.

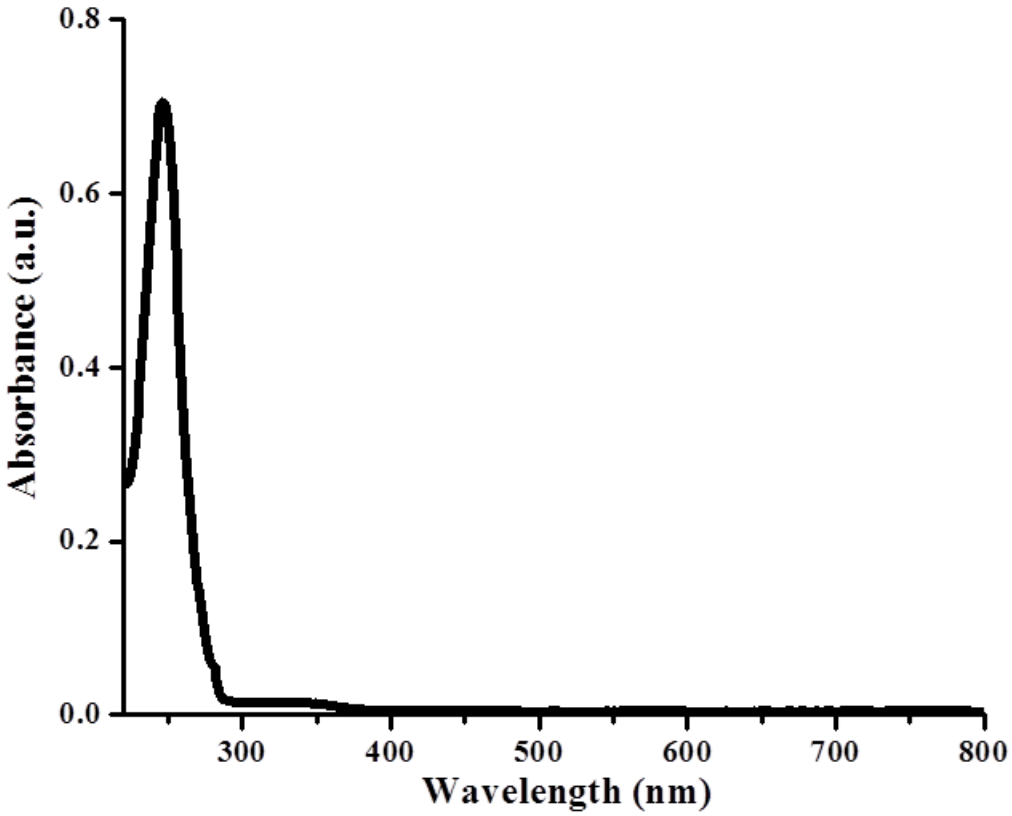

Fig. S5: The UV-Vis spectrum of ligand (L) solution.

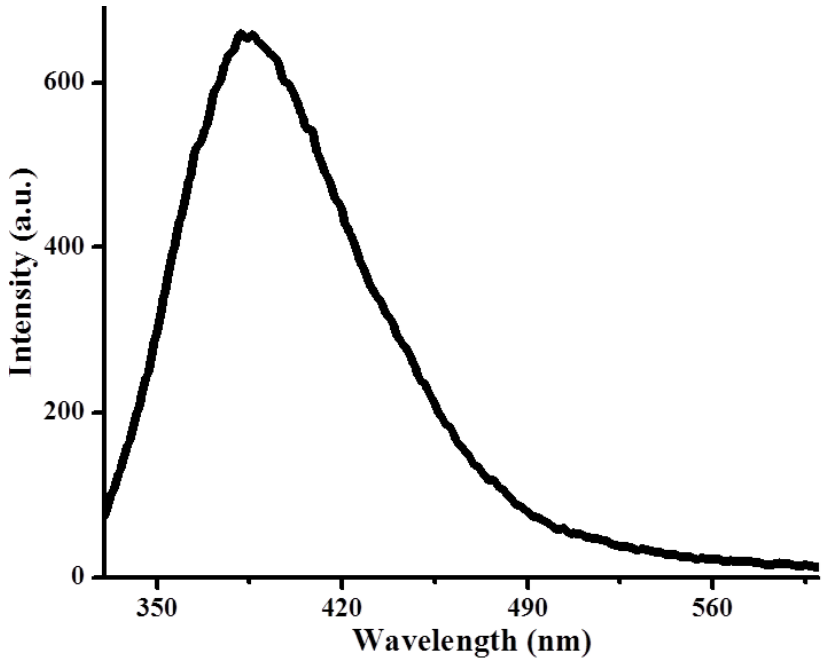

Fig. S6: The emission spectrum of ligand (L) solution excited at 315 nm.

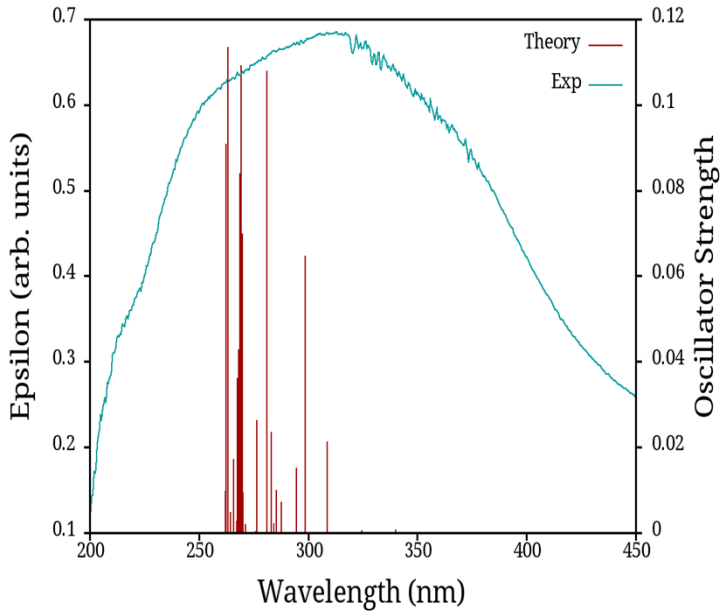

Fig. S7: The experimental (in solid state) and calculated UV-Vis spectrum of **1**.

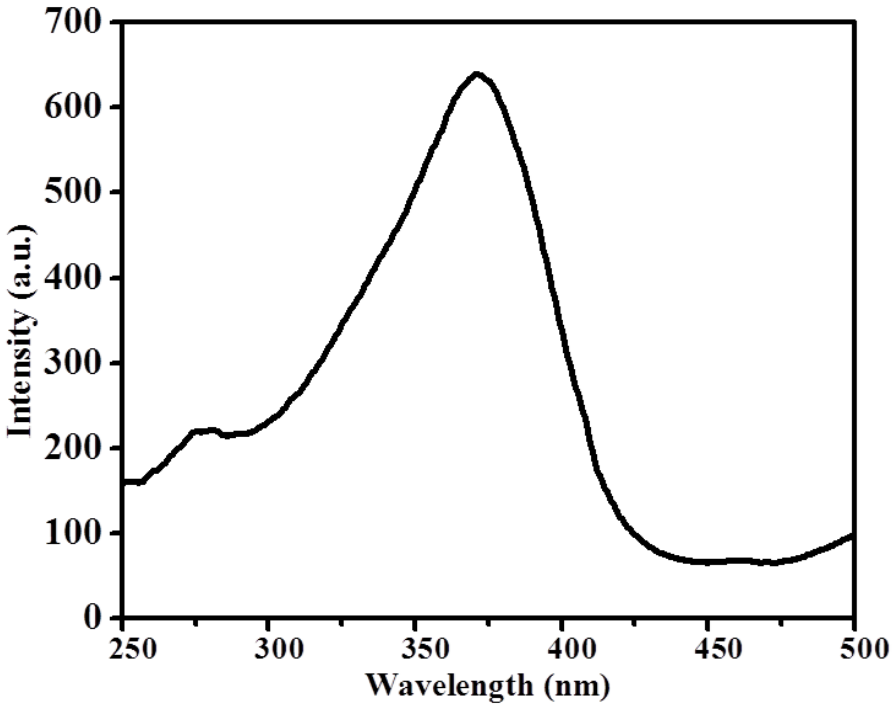

Fig. S8: The excitation spectrum of **1** in solid state monitoring the emission at 560 nm.

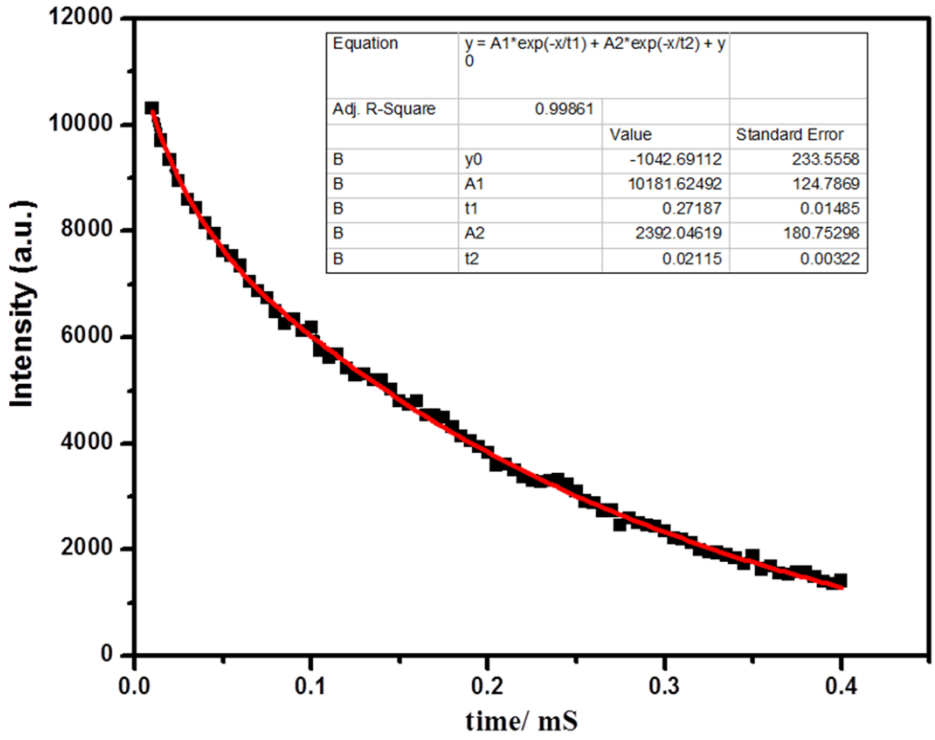

Fig. S9: Fluorescence lifetime decay profile of **1** (λ_{ex}=360 nm) while monitoring the emission at 560 nm

$$\tau_{adv} = \frac{\alpha_1\tau_1 + \alpha_2\tau_2}{\alpha_1 + \alpha_2}$$

$$\alpha_1 = \frac{A_1}{A_1 + A_2} = 0.8097$$

$$\alpha_2 = \frac{A_2}{A_1 + A_2} = 0.1902$$

τ_1= 0.2718 m sec

τ_2 = 0.0215 m sec

=224.1 μ sec

$$< \tau >= \frac{\alpha_1\tau_1 + \alpha_2\tau_2}{\alpha_1 + \alpha_2} = \frac{(0.8097 \times 0.2718) + (0.1902 \times 0.0215)}{0.8097 + 0.1902} = 0.2241 m \text{ sec}$$

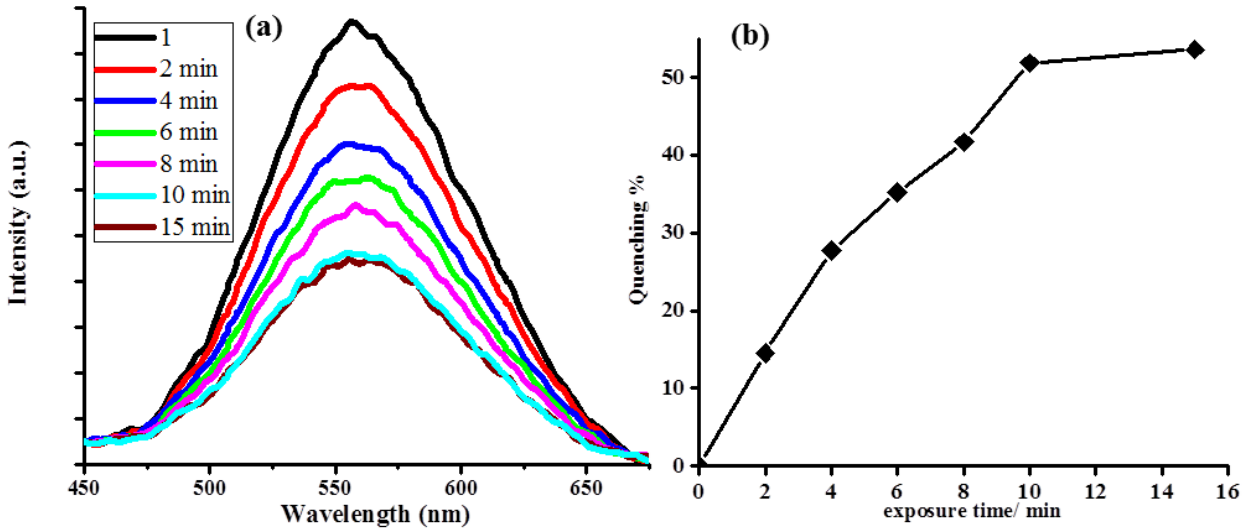

Fig. S10: Time dependent quenching of **1** in presence of *o*-DNB

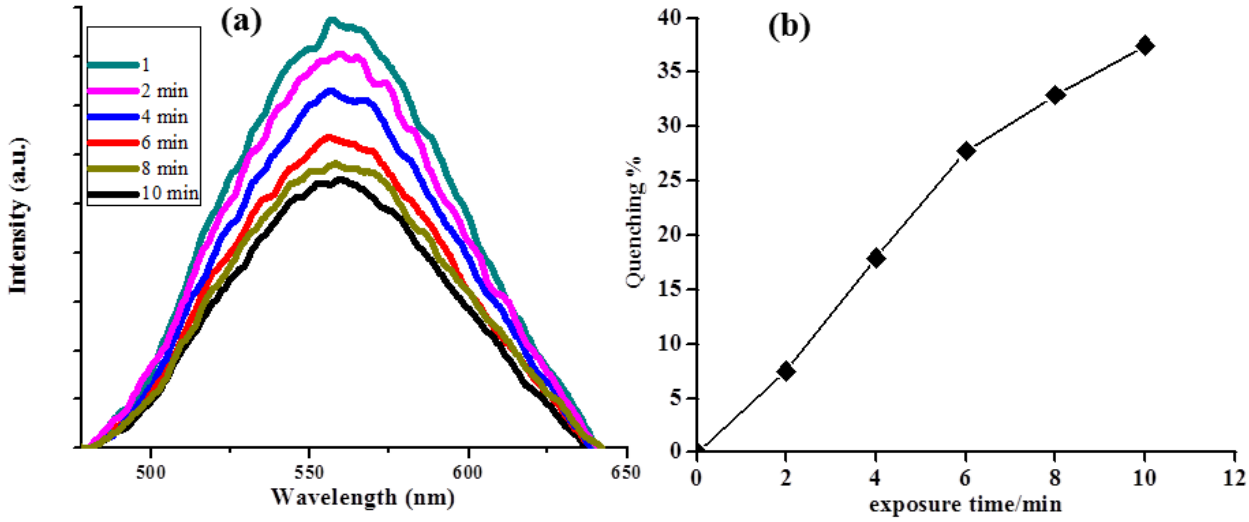

Fig. S11: Time dependent quenching of **1** in presence of DNT

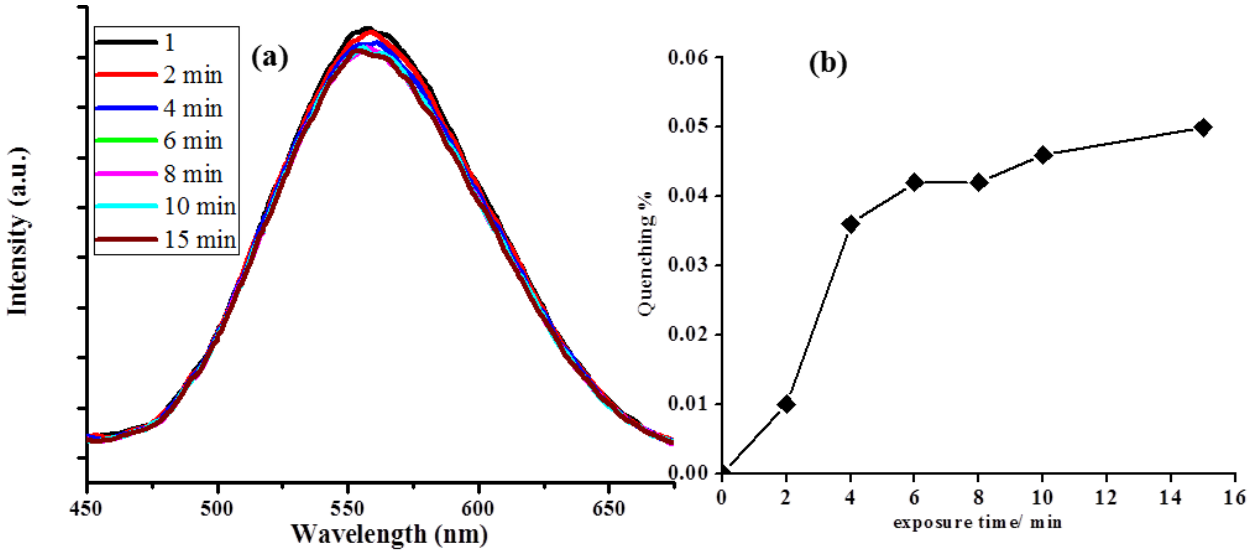

Fig. S12: Time dependent quenching of **1** in presence of nitromethane.

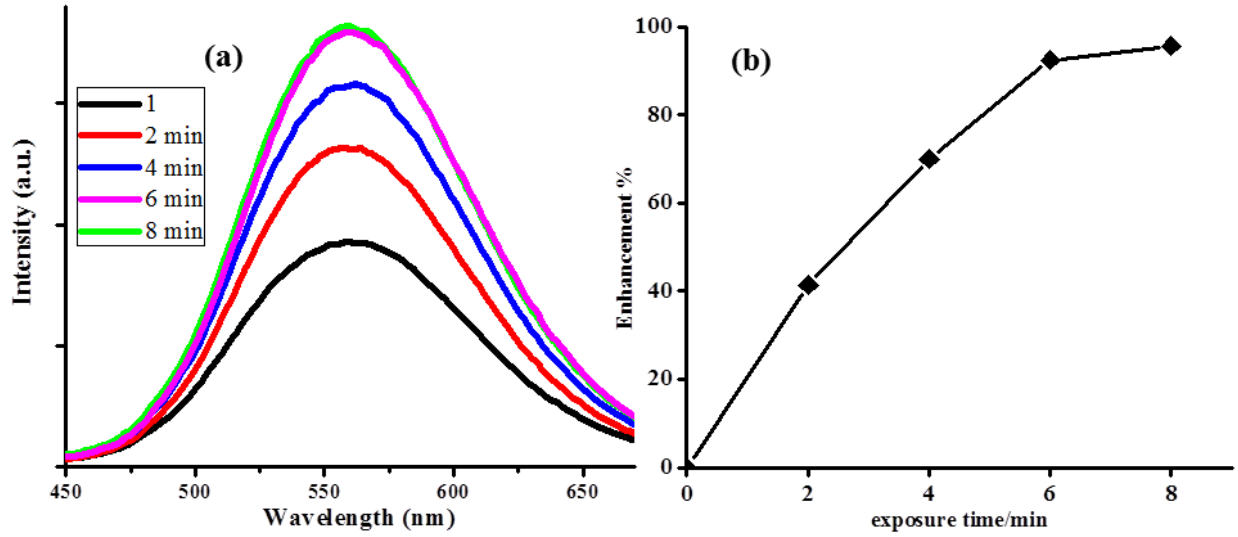

Fig. S13: Fluorescence enhancement of **1** in presence of toluene.

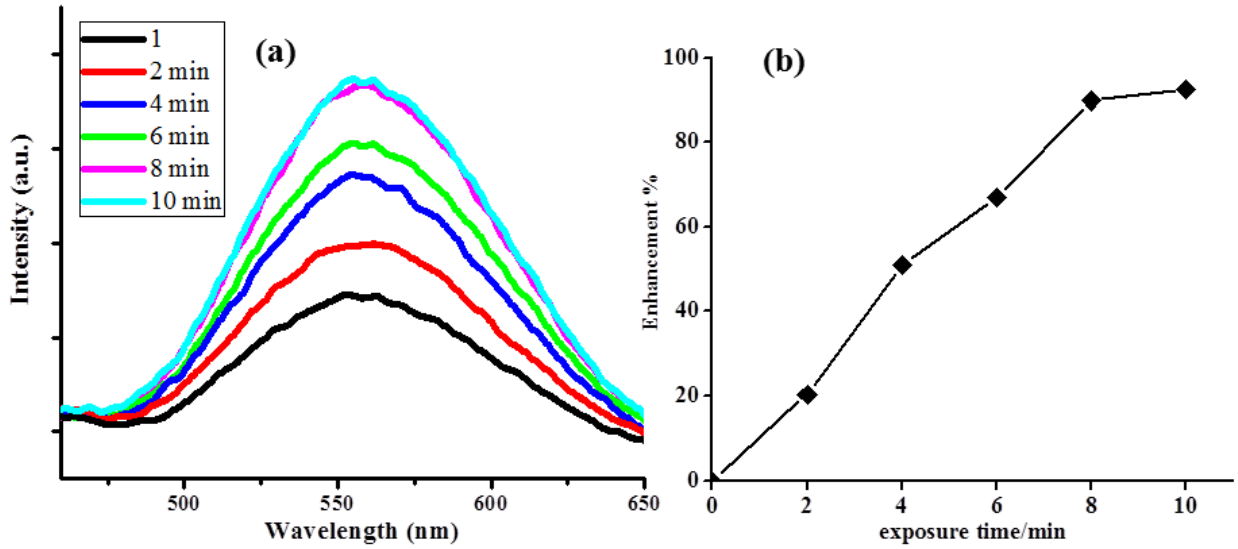

Fig. S14: Fluorescence enhancement of **1** in presence of *p*-xylene.

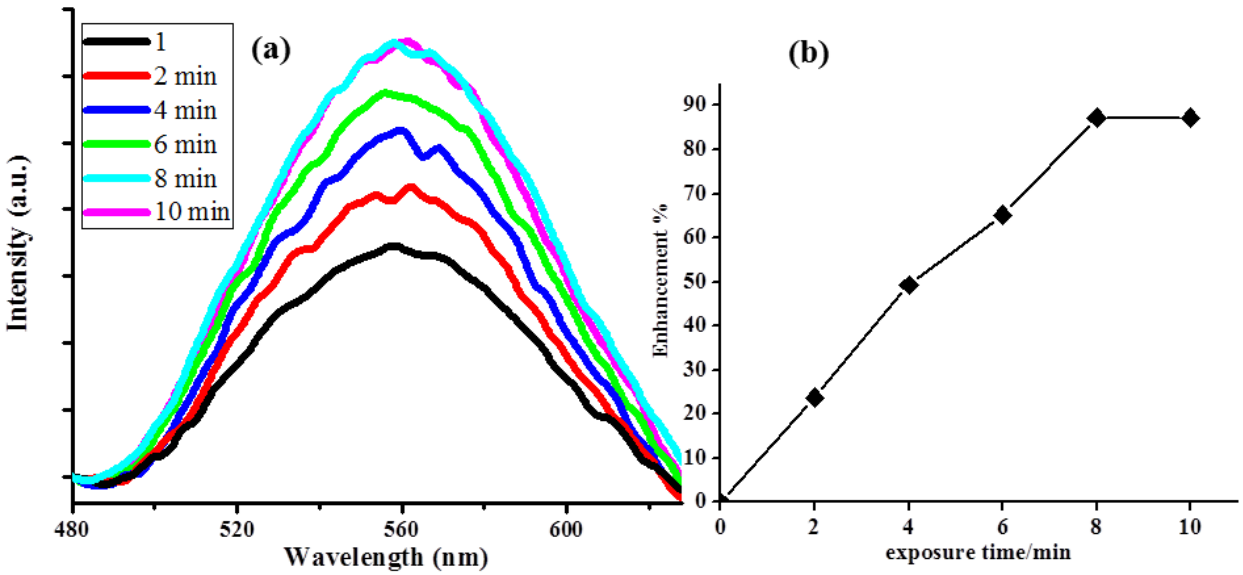

Fig. S15: Fluorescence enhancement of **1** in presence of *o*-xylene.

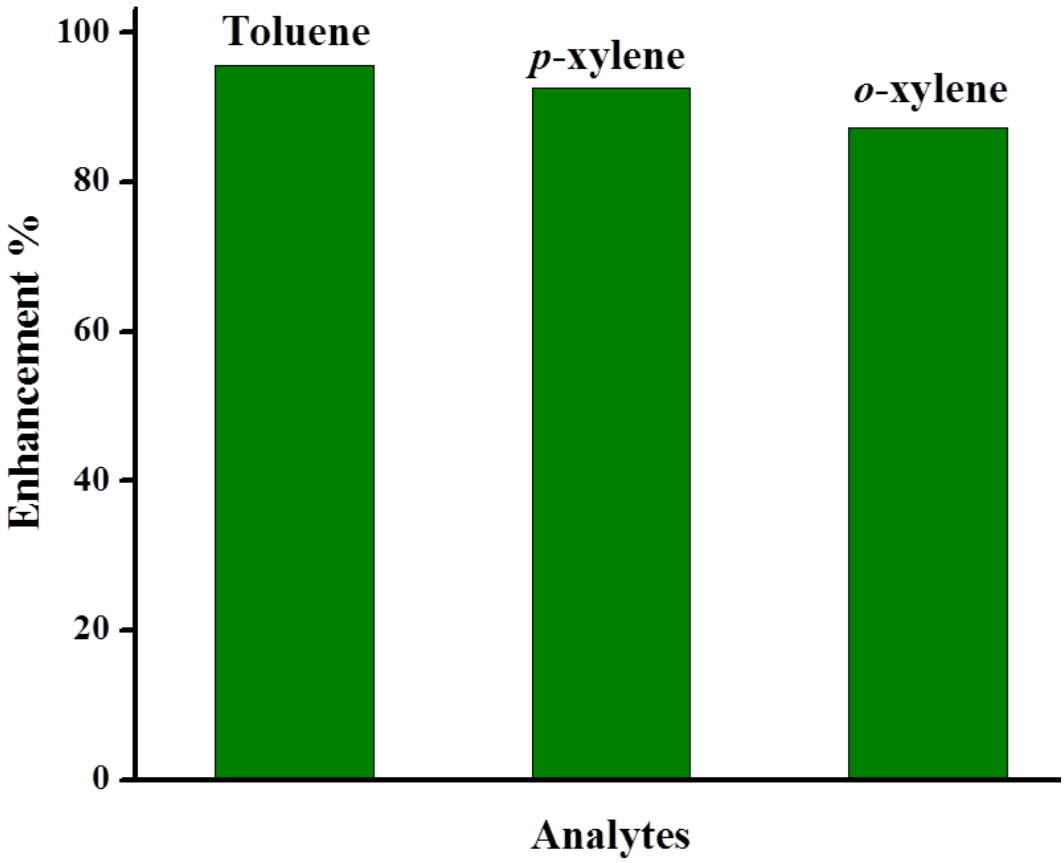

Fig. S16: Enhancement in fluorescence intensity observed upon the addition of different electron rich analytes.

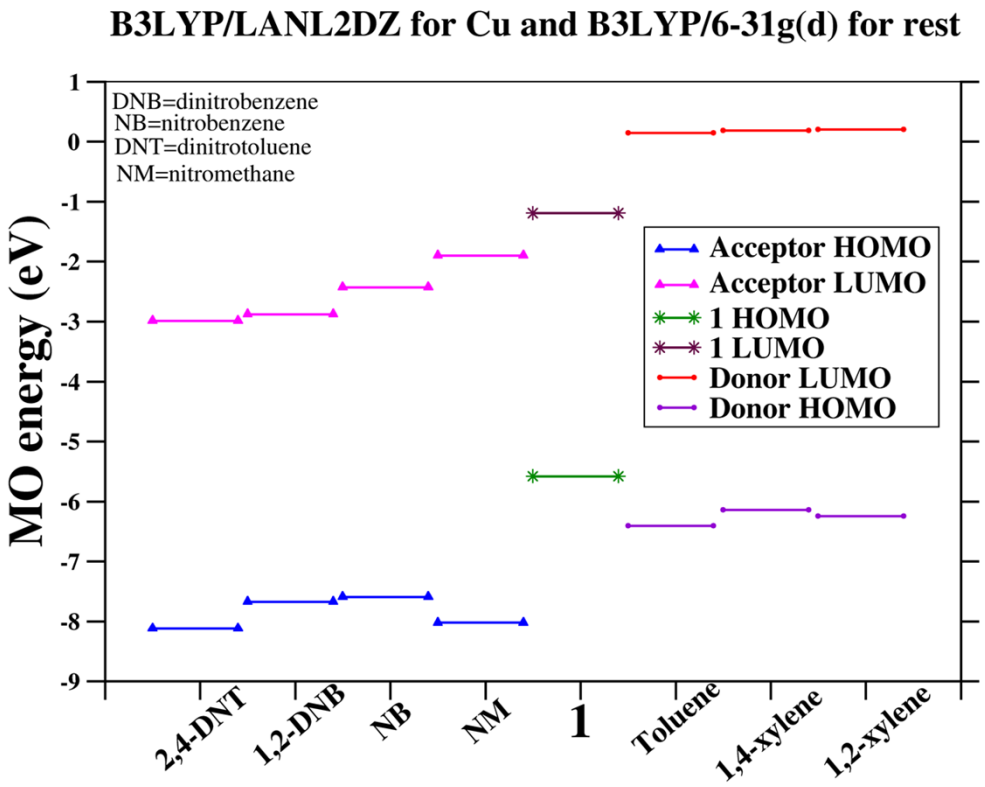

Fig. S17: Ordering of HOMO and LUMO energy levels of different analytes with respect to that of the parent compound **1.**

Table S1: Saturated Vapour Pressure for each of the analytes at room temperature (25 °C).

Analytes	Vapour pressure (mm Hg)
Nitrobenzene (NB)[5]	0.2416
o-dinitrobenzene (*o*-DNB)[6]	4.5×10^{-5}
2, 4-dinitrotoluene (DNT)[7]	1.44×10^{-4}
Nitromethane (NM)8	27.3
Toluene[9]	28.4
o-Xylene[10]	6.6
p-Xylene[10]	8.7

Table S2: Excitation nature of the important peaks (based on their oscillator strengths) and their wavelengths.

Excited state number	Wavelength (nm)	Osc. Strength	Excitation nature
6	308.63	0.0212	LMCT
8	298.62	0.0646	LMCT, MMCT, LLCT
10	294.53	0.0150	LMCT
18	283.16	0.0233	LMCT
19	281.08	0.1078	LMCT, MMCT, LLCT
20	281.06	0.0283	LMCT, MMCT, LLCT
23	276.39	0.0261	LMCT, LLCT
32	269.79	0.0697	LMCT, MMCT, LLCT
34	269.22	0.1090	LMCT, LLCT
36	268.69	0.0838	LMCT, MMCT, LLCT
37	268.18	0.0426	LMCT, LLCT
39	267.70	0.0359	LMCT, MMCT, LLCT
43	265.89	0.0170	LMCT
47	263.18	0.1134	LMCT, LLCT
49	262.51	0.0907	LMCT, LLCT

Table S3: Important distances of experimental and calculated triplet state geometries. Energies of triplet and singlet state (at triplet state geometry), emission wavelengths are also given.

Parameter	**Experimental**	**T1**	**Singlet at T1 geometry (S1)**
Cu-Cu distance range (Ang)	2.695-2.80	2.698-2.838	2.698-2.838
Cu-Cu average distance (Ang)	2.737	2.769	2.769
Cu-O distance range (Ang)	1.835-1.849	1.863-1.978	1.863-1.978
Cu-O average distance (Ang)	1.843	1.913	1.913
Energy (Har)		-4843.037	-4843.114
Emission (eV)	-	2.109	-
Emission (nm)	**560**	**587.830**	**-**

References:

1 (*a*) SMART (V 5.628), SAINT (V 6.45a), XPREP, SHELXTL; Bruker AXS Inc. Madison, Wisconsin, USA, 2004; (*b*) G. M. Sheldrick, Siemens Area Detector Absorption Correction Program, University of Göttingen, Göttingen, Germany, 1994; (*c*) A. Altomare, G. Cascarano, C. Giacovazzo and A. Gualaradi, *J. Appl. Cryst.*, 1993, **26**, 343; (*d*) G. M. Sheldrick, SHELXL-97, Program for Crystal Structure Solution and Refinement; University of Göttingen, Göttingen, Germany, 1997; (*e*) A. L. Spek, *J. Appl. Cryst.*, 2003, **36**, 7; (*f*) L.J. Farrugia, WinGX - A Windows Program for Crystal Structure Analysis. *J. Appl.Crystallogr.*, 1999, **32**, 837.

2 Gaussian 09, Revision B.01, M. J. Frisch, G. W. Trucks, H. B. Schlegel, G. E. Scuseria, M. A. Robb, J. R. Cheeseman, G. Scalmani, V. Barone, B. Mennucci, G. A. Petersson, H. Nakatsuji, M. Caricato, X. Li, H. P. Hratchian, A. F. Izmaylov, J. Bloino, G. Zheng, J.

L. Sonnenberg, M. Hada, M. Ehara, K. Toyota, R. Fukuda, J. Hasegawa, M. Ishida, T. Nakajima,Y. Honda, O. Kitao, H. Nakai, T. Vreven, J. A. Montgomery, Jr., J. E. Peralta, F. Ogliaro, M. Bearpark, J. J. Heyd, E. Brothers, K. N. Kudin, V. N. Staroverov, T. Keith, R. Kobayashi, J. Normand, K. Raghavachari, A. Rendell, J. C. Burant, S. S. Iyengar, J. Tomasi, M. Cossi, N. Rega, J. M. Millam, M. Klene, J. E. Knox, J. B. Cross, V. Bakken, C. Adamo, J. Jaramillo, R. Gomperts, R. E. Stratmann, O. Yazyev, A. J. Austin, R. Cammi, C. Pomelli, J. W. Ochterski, R. L. Martin, K. Morokuma, V. G. Zakrzewski, G. A. Voth, P. Salvador, J. J. Dannenberg, S. Dapprich, A. D. Daniels, O. Farkas, J. B. Foresman, J. V. Ortiz, J. Cioslowski, and D. J. Fox, Gaussian, Inc., Wallingford CT, 2010.

3 R. E. Stratmann, G. E. Scuseria and M. J. Frisch, *J. Chem. Phys*., 1998, **109**, 8218.

4 (*a*) F. D. Angelis, S. Fantacci, A. Sgamellotti, E. Cariati, R. Ugo and P. C. Ford *Inorg. Chem.*, 2006, **45**, 10576; (*b*) S. Perruchas, C. Tard, X. F. L. Goff, A. Fargues, A. Garcia, S. Kahlal, J.-Y. Saillard, T. Gacoin, and J.-P. Boilot *Inorg. Chem.*, 2011, **50**, 10682.

5 J.-S. Yang, T.M. Swager, *J. Am. Chem. Soc.*, 1998, **120**, 11864.

6 C.L. Yaws, Handbook of Vapor Pressure. Vol 2 C5-C7 Compounds. Houston, TX: Gulf Publ Co, 1994, 391.

7 A. Lan, K. Li, H. Wu, D. H. Olson, T. J. Emge, W. Ki, M. Hong, J. Li, *Angew.Chem. Int. Ed.*, 2009, **48**, 2334.

8 *CRC Handbook of Chemistry and Physics* 44th ed.

9 http://www.epa.gov/ttn/atw/hlthef/toluene.html.

10 http://scorecard.goodguide.com/chemical-profiles/html/xylenes.html.